Published in IEEE Journal of Selected Topics in Quantum Electronics 8, issue 1, 46-57, 2002
which should be used for any reference to this work

Microoptical Fiber Switch for a Large Number of Interconnects: Optical Design Considerations and Experimental Realizations Using Microlens Arrays

Yves-Alain Peter, Hans Peter Herzig, and René Dändliker

***Abstract*—The authors investigate a $1 \times N$ free-space microoptical fiber switch for a large number of interconnects. The system to be studied is a reflective $4f$ optical system. Alignment tolerances and coupling efficiency are investigated and the benefit brought by collimating microlens arrays is reported (theoretically and experimentally). The use of microlenses enables power coupling efficiency between 3 and 2 dB (including losses due to the optical elements) for an optical switch allowing up to 3000 receiver fibers.**

***Index Terms*—Fiber, microlens, MOEMs, optical switch.**

I. Introduction

DURING the past few years, the demand for optical telecommunications has boomed [1]. In order to satisfy this demand, new optical switches are required to replace the electrical switches used until now. Optical switches with a few interconnects (1×2, or 2×2) have been published recently [2]. In the future, optical telecommunication networks need optical switches with a large number of interconnects. Alignment tolerances, diffraction of the beams, and aberrations are more critical for optical switches witha large number of interconnects than for optical switches with a few interconnects. In this paper, we present a study of the main issues of the optical system for a large number of interconnects. Both theoretical investigations based on ray tracing and power coupling efficiency as well as experiments are shown. In Sections III–VI, we present the basic concepts (aberrations, power coupling efficiency calculations, alignment tolerances, and effect of aperture). Section VII-C details investigations of the above-mentioned basic concepts for a specific *study* optical switching system. In Section VIII, we show the advantages of using collimating microlens arrays. Section IX presents the experimental results of both systems, with and without collimating microlens arrays.

II. General Concept

The optical system has two functions. First, it images a singlemode source fiber onto a singlemode receiver fiber (coupling function). Second, it deflects the beam to address one of the receiver fibers (switching function). Fig. 1 shows such a system composed of a fiber bundle, a lens, and a mirror. The source fiber is imaged ($4f$ system) onto one of the receiver fibers by moving the lens laterally. There are of course other possibilities to switch the light. The system serves as a representative example to study the interconnect problems.

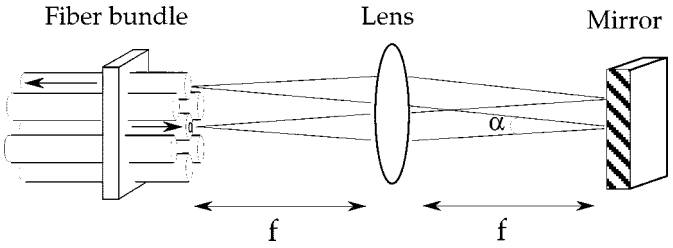

Fig. 1. Schematic setup of the free-space optical switching system.

III. Aberrations

In geometrical optics, light is assumed to consist of rays. The chief ray is defined as the ray from an object point which passes through the center of the aperture stop and the center of both entrance and exit pupils (see Fig. 2). If rays emerging from the object point P are traced through the optical system up to the exit pupil such that each one travels an optical path length equal to that of the chief ray, the surface passing through their end points is called the system wavefront for the object point under consideration. If the wavefront is spherical, we say that the image is perfect; else, the image is aberrated. The deviations of the optical path length (i.e., geometric deviations times the refractive index n_i of the image space) of the wavefront from the reference sphere in the pupil plane are called wave aberrations W (see Fig. 2).

IV. Power Coupling Efficiency

The merit function of an optical fiber switch is its coupling efficiency. We will here briefly summarize the calculation method of the power coupling efficiency. Considering the source wave function ϕ, we compute the source efficiency

$$\eta_P = \frac{\iint_{P(x,y)} \phi(x, y)\phi^*(x, y)\, dx\, dy}{\int_{-\infty}^{\infty}\int_{-\infty}^{\infty} \phi(x, y)\phi^*(x, y)\, dx\, dy} \tag{1}$$

Y.-A. Peter was with the Institute of Microtechnology, University of Neuchâtel, Neuchâtel, Switzerland. He is now with the Microphotonics Laboratory, Stanford University, Stanford, CA 94305 USA (e-mail: yap@ieee.org).

H. P. Herzig and R. Dändliker are with the Institute of Microtechnology, University of Neuchâtel, Neuchâtel, Switzerland.

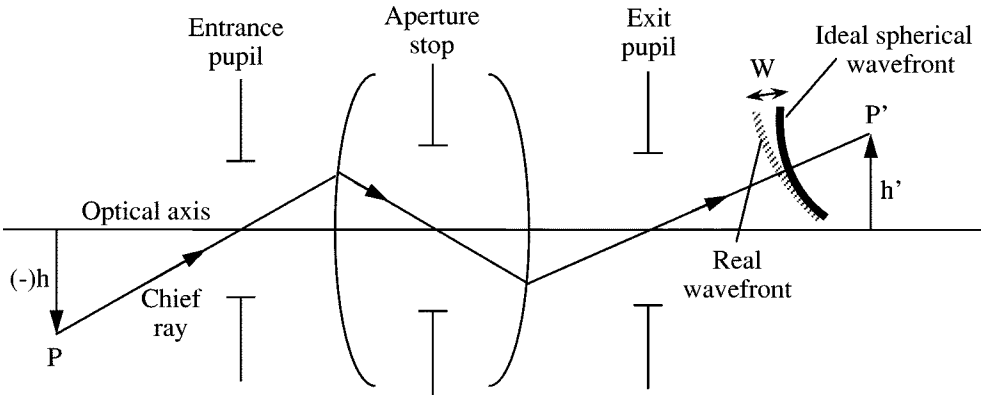

Fig. 2. Schematic of an optical imaging system.

which is the normalized power collected by the entrance pupil of the optical system. The integral in the numerator is taken over the aperture of the system given by the pupil function $P(x, y)$. The (*) symbol represents the complex conjugate. Then, we compute the power-coupling efficiency

$$\eta = \frac{\left| \int_{-\infty}^{\infty}\int \phi'(x, y)\psi^*(x, y)\, dx\, dy \right|^2}{\int_{-\infty}^{\infty}\int \phi'(x,y)\phi'^*(x,y)\, dx\, dy \int_{-\infty}^{\infty}\int \psi(x,y)\psi^*(x,y)\, dx\, dy} \tag{2}$$

which is the normalized overlap integral of the incident wave function $\phi'(x, y)$ illuminating the receiver fiber and the modal wave function $\psi(x, y)$ of the receiver fiber. The wave function ϕ' is given by

$$\phi' = h \circ \phi \tag{3}$$

where h is the impulse response or amplitude point-spread function (APSF) of the system, ϕ is the wave function of the source fiber, and the $\circ$ symbol represents the convolution. The impulse response h is proportional to the Fourier transform of the generalized pupil function $\mathcal{P}(\xi, \zeta)$ [3]

$$h \propto FT\{\mathcal{P}(\xi, \zeta)\}. \tag{4}$$

The generalized pupil function is defined by

$$\mathcal{P}(\xi, \zeta) = P(\xi, \zeta)e^{ikW(\xi,\zeta)} \tag{5}$$

where $W(\xi, \zeta)$ is the function describing the aberrations (see Section III).

Finally, the total power coupling efficiency is

$$\eta_{tot} = \eta_P \eta. \tag{6}$$

V. Alignment Tolerances

The effect of fiber misalignment (lateral, longitudinal, and tilt) (see Fig. 3) on the power coupling efficiency between one source fiber and one receiver fiber can be calculated using (2) [4]. The receiver fiber mode at the receiver fiber plane is given, in a good approximation, by the complex amplitude

$$\psi(x, y) = \exp\left[-\frac{x^2 + y^2}{w_r^2}\right] \tag{7}$$

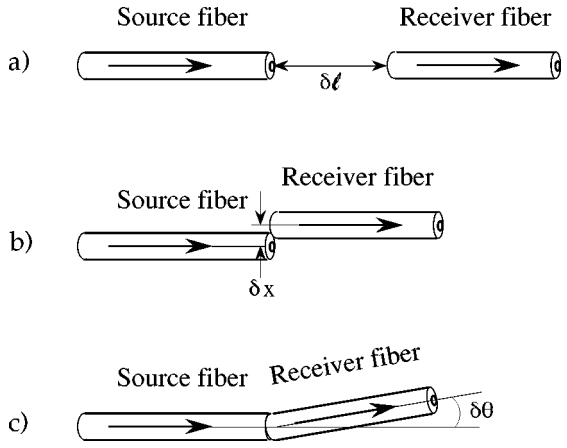

Fig. 3. Misalignments for coupling light from a source fiber into a receiver fiber: a) longitudinal offset, b) lateral offset, and c) tilt.

with w_r the waist of the Gaussian mode of the receiver fiber at the receiver fiber plane. For a longitudinal misalignment δl, the mode $\phi'_{\delta l}(x, y)$ at the receiver fiber plane becomes

$$\phi'_{\delta l}(x, y) = \exp\left[-\frac{x^2 + y^2}{w_2^2(\delta l)}\right] \tag{8}$$

with $w_2(\delta l)$ given by

$$w_2(\delta l) = w_2\sqrt{1 + \left(\frac{\delta l}{z_0}\right)^2} \tag{9}$$

where z_0 is the Rayleigh range. The coupling efficiency between two identical fibers ($w_s = w_r = w$) is then given, using (2), by

$$\eta_{\delta l} = \frac{(\delta l/z_0)^2 + 1}{\frac{1}{4}(\delta l/z_0)^4 + (\delta l/z_0)^2 + 1}. \tag{10}$$

Fig. 4 shows how the power coupling efficiency decreases with increasing fiber distance δl in terms of $z_0 = \pi w^2/\lambda$ using (10). For $w = 2.25$ μm and $\lambda = 633$ nm ($z_0 = 25.13$ μm), a longitudinal offset of 30 μm generates 1 -dB insertion loss (80% coupling efficiency).

For a lateral misalignment δx, the mode $\phi'_{\delta x}(x, y)$ becomes

$$\phi'_{\delta x}(x, y) = \exp\left[-\frac{(x + \delta x)^2 + y^2}{w_s^2}\right]. \tag{11}$$

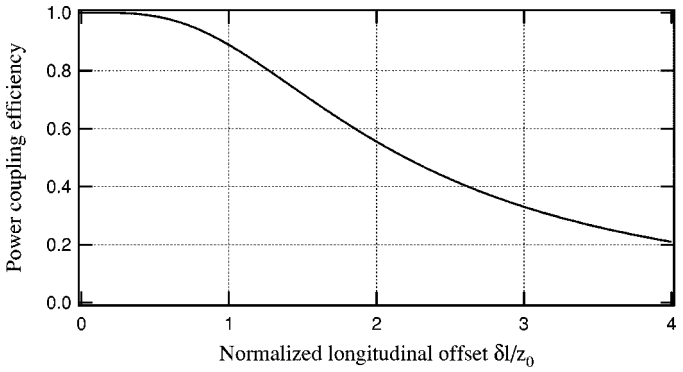

Fig. 4. Power coupling efficiency between two identical singlemode fibers versus normalized longitudinal misalignment $\delta l/z_0$.

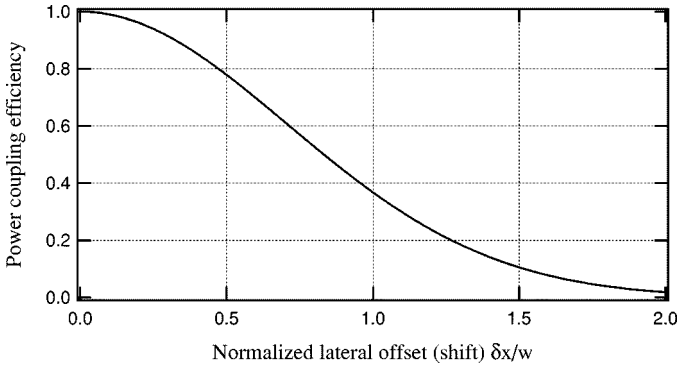

Fig. 5. Power coupling efficiency between two identical singlemode fibers versus normalized lateral offset $\delta x/w$.

The coupling efficiency between two identical fibers ($w_s = w_r = w$) is then given, using (2), by

$$\eta_{\delta x} = \exp\left(-\frac{\delta x^2}{w^2}\right). \tag{12}$$

Fig. 5 shows how the power coupling efficiency decreases with increasing lateral offset δx between the two fibers using (12) in terms of the Gaussian beam width w. For $w = 2.25$ μm, a lateral offset of 1 μm generates 1-dB insertion loss (80% coupling efficiency).

Finally, an angular misalignment $\delta\theta$ between two identical fibers ($w_s = w_r = w$) produces a linear phase change across the beam on the receiver fiber. The mode $\phi'_{\delta\theta}(x, y)$ can be described by

$$\phi'_{\delta\theta}(x, y) = \exp\left[-\frac{x^2+y^2}{w_s^2}\right]\exp\left[x\,\frac{-2\pi i}{\lambda}\tan\delta\theta\right]. \tag{13}$$

Using (2), the coupling efficiency is given by

$$\eta_{\delta\theta} = \exp\left[-\left(\frac{\tan\delta\theta}{\theta_0}\right)^2\right] \cong \exp\left[-\left(\frac{\delta\theta}{\theta_0}\right)^2\right] \tag{14}$$

with $\theta_0 = \lambda/\pi w_0$, the angular divergence of the Gaussian beam. Fig. 6 shows how the power coupling efficiency decreases with increasing angular misalignment between the two fibers $\delta\theta$ in terms of divergence $\theta_0 = \lambda/\pi w_0$ of the Gaussian beam using (14). For $w = 2.25$ μm and $\lambda = 633$ nm ($\theta_0 = 5.14°$), a tilt of 2.4° generates 1-dB insertion loss (80% coupling efficiency).

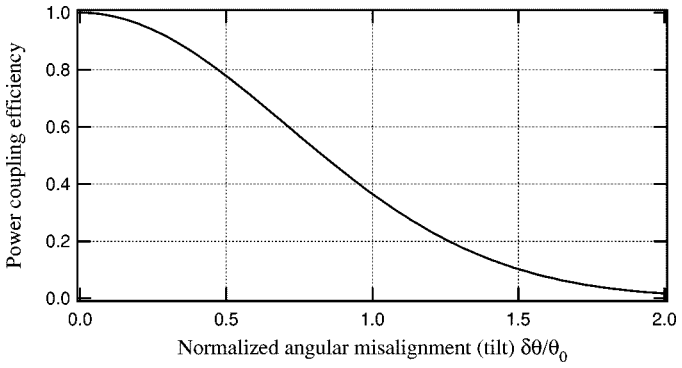

Fig. 6. Power coupling efficiency versus normalized angular misalignment $\delta\theta/\theta_0$ between two identical singlemode fibers.

From the above calculations, we see that longitudinal alignment is less critical than lateral or angular alignment.

VI. Aperture of the Optical System

In a fiber coupling system, the effect of a stop, given by its radius $r_{\max}$, has two effects. First, the stop will cut a part of the propagating beam (loss accounted in η_P; see Section IV). Second, the aperture will cause an image broadening due to diffraction (the wave function ϕ' in (2) differs from the source wave function ϕ and the coupling efficiency η is reduced). The two effects are cumulative. In the following, we discuss the losses due to finite stops and we determine the ratios $r_{\max}/w(z)$ needed to get an acceptable coupling efficiency.

Let us consider the simple case where the optical coupling system has a single lens with a stop of radius $r_{\max}$. The total power coupling efficiency η_{tot} introduced in Section IV can be simplified and computed at the plane of the lens. Let $\phi(x, y)$ and $\psi(x, y)$ be the source and receiver fiber modes, respectively, given by the following Gaussian profile:

$$\exp\left[-\frac{x^2+y^2}{w^2}\right]. \tag{15}$$

The total power coupling efficiency expressed in polar coordinates is

$$\begin{aligned}\eta_{tot} &= \frac{\left|\displaystyle\int_0^{r_{\max}} e^{-2(\rho^2/w^2)}\rho\,d\rho\right|^2}{\displaystyle\int_{-\infty}^{\infty} e^{-2(\rho^2/w^2)}\rho\,d\rho \int_{-\infty}^{\infty} e^{-2(\rho^2/w^2)}\rho\,d\rho} \\ &= \left[1 - e^{-2(r_{\max}^2/w^2)}\right]^2 \end{aligned} \tag{16}$$

with $\rho^2 = x^2 + y^2$. As can be seen in Fig. 7, the coupling efficiency η is better than 98% for $r_{\max}/w(z) \geqslant 1.5$. In terms of the numerical apertures of the optics (NA_{lens}) and of the source fiber (NA_{fiber}), this condition can also be expressed as $NA_{\text{lens}} \geqslant 1.5NA_{\text{fiber}}$. This condition can be considered as a rule of thumb for any optical fiber switch.

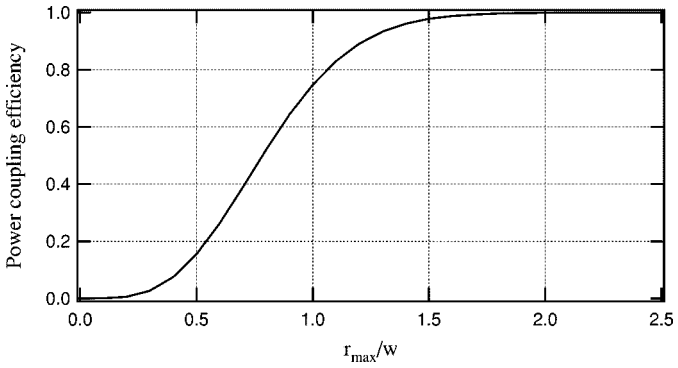

Fig. 7. Effect of the aperture size on the coupling efficiency ($2r_{\max}$ = diameter of the aperture and $2w$ = diameter of the Gaussian beam).

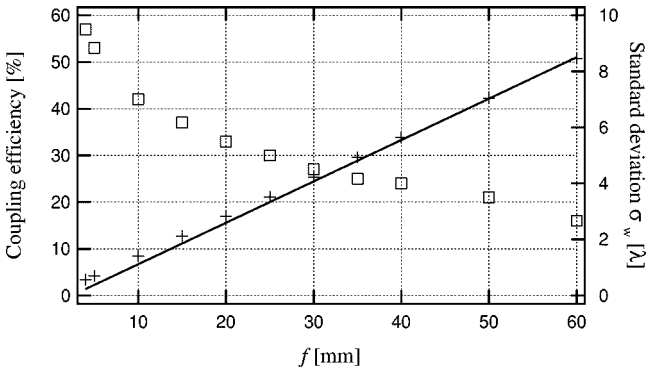

Fig. 8. Power coupling efficiency (□) and standard deviation σ_W (+) of the aberration function W versus focal length f of the plano-convex lens (BK7: $n = 1.52$ at 633 nm) with a numerical aperture $NA_{\text{lens}} = 0.17$.

VII. Simulations of the Switching System

In this section, the aberrations of a real lens will play a central role. The characteristics of the lens will be discussed regarding their influence on the power coupling efficiency. An important part of this section is dedicated to the dependence of the aberrations on the optical system. Several system designs are numerically analyzed using different values for the aperture of the lens, the focal length, and the size of the system.

Calculations of the power coupling efficiency will be done based on the method described in Section IV. The point spread function h is calculated by the ray tracing program Zemax. The incident wave function ϕ' illuminating the receiver fiber is calculated using (3). The power coupling efficiency is then obtained by computing the normalized overlap integral of (2).

The system is composed of a source fiber, a lens, and a mirror. The source fiber is imaged ($4f$ system) onto one of the receiver fibers by moving the lens laterally as shown in Fig. 1. We use a flat mirror and investigate the aberrations of the system. The choice of the lens is important, since the lens is the main source of aberrations in the system.

For rotationally symmetric elements, only spherical aberration can occur on axis (object height $h = 0$). The spherical aberrations are proportional to the power of 4 of the numerical aperture and proportional to the focal length [5], [6]

$$W_{\text{sph}} \sim NA^4 f. \tag{17}$$

It means that reducing the size of the lens will reduce the aberrations to the power of 4. It means also that reducing the focal length will decrease the aberrations proportionally. Note that it is not possible (due to fabrication limitations) to make the size of the lens arbitrarily small and keep the same focal length. It is also not possible to reduce the focal length below a certain limit, if we want to address a large number of receiver fibers and keep the deflection angles α relatively small (see Fig. 1).

A. Effect of Aberrations for Different Lenses On-Axis

In order to investigate the influence of the aberrations in our system, we simulate the $4f$ system using the ray tracing program Zemax. Two values will be investigated: the standard deviation σ_W of the aberrations W given by

$$\sigma_W^2 = \langle W^2(\rho,\theta)\rangle - \langle W(\rho,\theta)\rangle^2 \tag{18}$$

and the power coupling efficiency. The aberrations are computed over the entire aperture of the optical system given by NA_{lens}.

1) Plano-Convex Lenses: First, we consider a plano-convex lens. As an example, a commercially available plano-convex lens made of BK7 ($n = 1.52$ at 633 nm) was chosen. Fig. 8 shows the dependence of the standard deviation σ_W of the aberrations and the power coupling efficiency as a function of the focal length f of the plano-convex lens in the on-axis position. The numerical aperture of the fibers is $NA_{\text{fiber}} = 0.11$ and the numerical aperture of the lens is chosen as $NA_{\text{lens}} = 1.5NA_{\text{fiber}} = 0.17$ to satisfy the criterion given in Section VI. We see in Fig. 8 the linear dependence of the aberrations (standard deviation σ_W) with the focal length f as expected from (17). The smaller the focal length, the smaller the aberrations, thus the higher the power coupling efficiency. However, the efficiency here is quite poor, even for very small focal lengths. This is due to the aberrations which remain important, even for small focal length ($\sigma_W = 0.6$ for $f = 4$ mm). In order to have the maximum coupling efficiency, the system should be diffraction limited. This means that the performance of the system is limited by the physical effects of diffraction rather than by the aberrations. Let us consider the *Strehl ratio* [7]

$$\text{Strehl ratio} \simeq 1 - \left(\frac{2\pi}{\lambda}\right)^2 \sigma_W^2 \cong \eta \tag{19}$$

which is the illumination at the center of the airy disc for an aberrated system expressed as a fraction of the corresponding illumination for a perfect system. The Strehl ratio is a good approximation for the coupling efficiency η valid for small aberrations only. An ideal system has a Strehl ratio of 1. A Strehl ratio of 0.8 corresponds to a peak to value wavefront error W of around $\lambda/4$ and to a standard deviation of $\sigma_W = 0.07\lambda$.

In Fig. 8 we see that a focal length $f = 6$ mm of the plano-convex lens corresponds to a coupling efficiency of 50% (3 -dB insertion loss). Such a focal length is, however, too small to address a large number of receiver fibers in a switching configuration (lens off-axis) while keeping the deflection angle α relatively small (see Fig. 1). The low values obtained for the coupling efficiency of the system using a plano-convex lens are even worse if the lens is placed with its curved surface facing

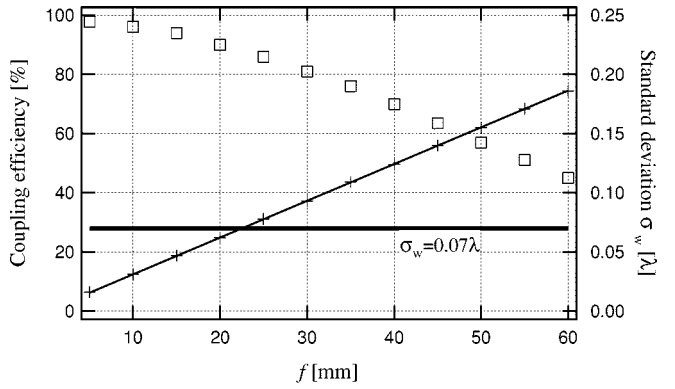

Fig. 9. Power coupling efficiency (□) and standard deviation σ_W (+) of the aberration function W versus focal length f of the achromat. The achromat is a doublet made of SF2 ($n = 1.64$ at 633 nm) and BK7 ($n = 1.52$ at 633 nm) and has a numerical aperture $NA_{\rm lens} = 0.17$.

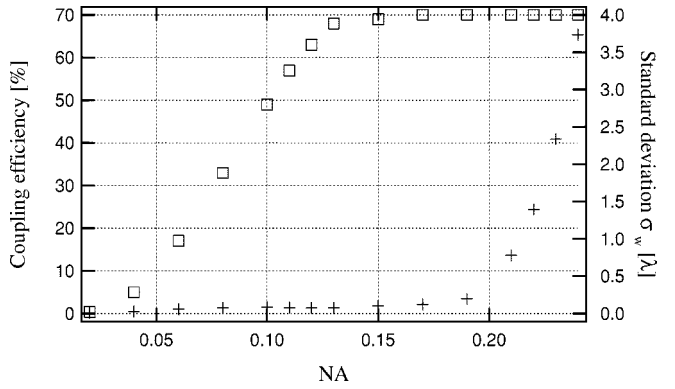

Fig. 10. Power coupling efficiency (□) and standard deviation σ_W (+) of the aberration function W versus numerical aperture $NA_{\rm lens}$ of the achromat. The achromat is a doublet made of SF2 ($n = 1.64$ at 633 nm) and BK7 ($n = 1.52$ at 633 nm) and has a focal length $f = 40$ mm.

the fibers. Effectively, placing the plano-convex lens with the curved surface facing the fibers makes the rays undergo one large refraction instead of two small refractions. For a focal length $f = 40$ mm, $\sigma_W = 5.6$ and the coupling efficiency is 23% if the lens is placed with the flat surface facing the fibers, and $\sigma_W = 22$ and the coupling efficiency is 10% if the lens is placed with the curved surface facing the fibers.

2) Achromats: The use of an achromat instead of a plano-convex lens is a better choice in order to have small aberrations. The chosen achromat is a commercially available doublet (Linos #322 209) made of SF2 ($n = 1.64$ at 633 nm) and BK7 ($n = 1.52$ at 633 nm). Fig. 9 shows the dependence of the standard deviation σ_W of the aberrations and the power coupling efficiency as a function of the focal length f of the scaled achromat. The numerical aperture of the lens is $NA_{\rm lens} = 0.17$ and the numerical aperture of the fibers is $NA_{\rm fiber} = 0.11$. We see again the linear dependence of the aberrations (standard deviation σ_W) on the focal length f. The efficiency here is much higher than for a plano-convex lens. For a focal length $f \lesssim 30$ mm, the insertion loss is less than 1-dB (power coupling efficiency higher than 80%). Fig. 10 shows the dependence of the standard deviation σ_W of the aberrations and the power coupling efficiency as a function of the numerical aperture $NA_{\rm lens}$ of the achromat. The focal length $f = 40$ mm and the numerical

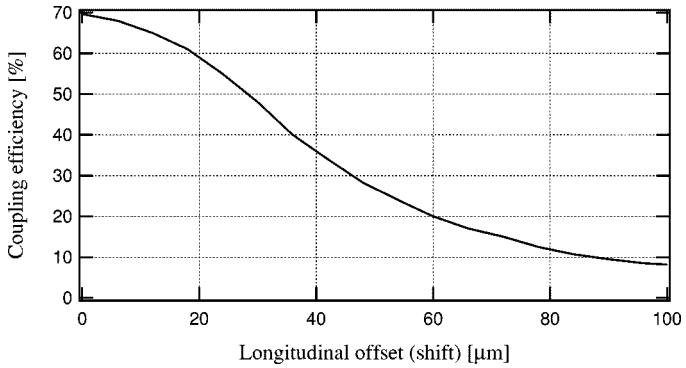

Fig. 11. Power coupling efficiency for the $4f$ system with the achromat on-axis versus longitudinal misalignment of the receiver fiber ($f = 40$ mm, $NA_{\rm fiber} = 0.11$, $NA_{\rm lens} = 0.17$).

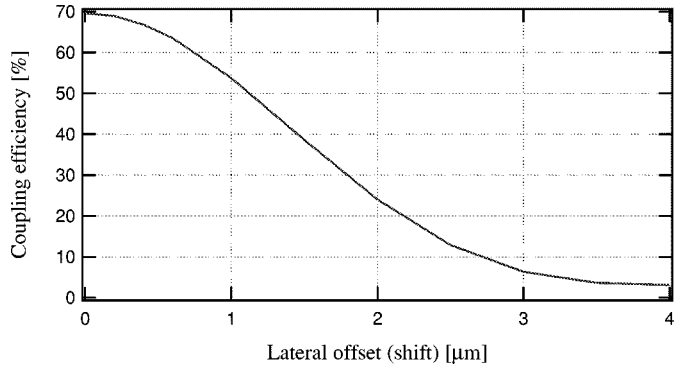

Fig. 12. Power coupling efficiency for the $4f$ system with the achromat on-axis versus lateral misalignment of the receiver fiber ($f = 40$ mm, $NA_{\rm fiber} = 0.11$, $NA_{\rm lens} = 0.17$).

aperture of the fibers is $NA_{\rm fiber} = 0.11$. For small $NA_{\rm lens}$, the power coupling efficiency drops due to the clipping effect. This effect begins to influence the power coupling efficiency as soon as $NA_{\rm lens} \lesssim 1.5 NA_{\rm fiber}$ as already discussed in Section VI. For large $NA_{\rm lens}$, the increasing aberrations of the lens have no influence on the power coupling efficiency, since most of the intensity is within the limit $NA_{\rm lens} \lesssim 1.5 NA_{\rm fiber}$. The insertion loss approaches a limit of 1.5 dB ($\eta = 70\%$).

B. Alignment Tolerances for an Achromat On-Axis

The tolerances for longitudinal offset (Fig. 11), lateral offset (Fig. 12), and for angular misalignment (Fig. 13) of the receiver fiber with the achromat on-axis and the flat mirror are quite similar to those calculated for simple coupling between two fibers (see Figs. 4–6, respectively).

The lateral offset of the receiver fiber can be corrected by displacing the achromat laterally or by adjusting the distance between the achromat and the flat mirror (see Fig. 1). If we consider a 1-dB additional insertion loss (56% coupling efficiency in Fig. 12), the lateral tolerance on the receiver fiber is $\delta x = 1$ μm. Since the beam displacement on the receiver fiber is twice the lateral displacement of the lens, the corresponding tolerance for a lateral offset of the achromat is $\delta x/2 = 0.5$ μm.

C. Switching: Achromat Off-Axis

Placing the achromat off-axis as shown in Fig. 14 enables us to connect the receiver fibers. Fig. 15 shows the coupling

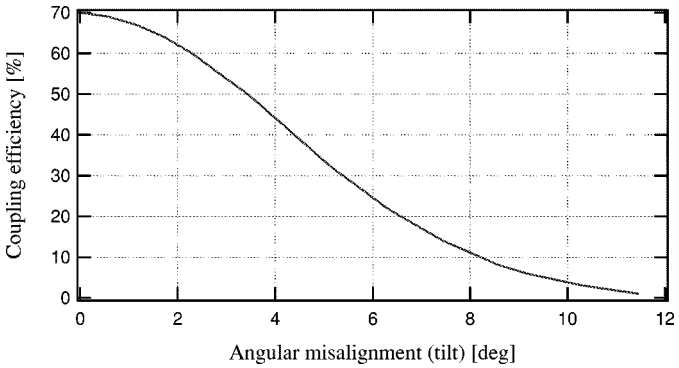

Fig. 13. Power coupling efficiency for the $4f$ system with the achromat on-axis versus angular misalignment of the receiver fiber ($f = 40$ mm, $NA_{\text{fiber}} = 0.11$, $NA_{\text{lens}} = 0.17$).

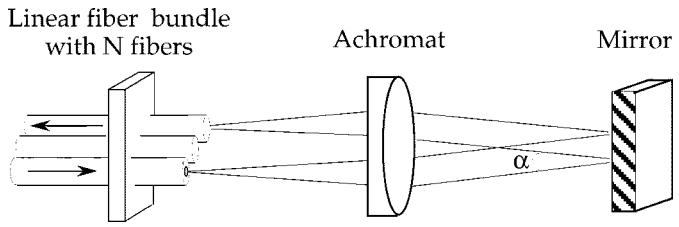

Fig. 14. Setup of a 1-D one-directional $4f$ system with one achromat and a flat mirror ($f = 40$ mm, $NA_{\text{fiber}} = 0.11$, $NA_{\text{lens}} = 0.17$).

efficiency for different switching configurations using an achromat. The top solid line is for 1–to–1 coupling (source and receiver fiber are the same, achromat on-axis). The other lines are for one-dimensional (1-D) one-directional switching configurations 1×1, 1×2, 1×3, 1×4, 1×5, 1×6, 1×7, and 1×8 from second top to last bottom traces. For the 1×1 switching configuration (receiver fiber next to source fiber), the achromat is shifted 0.125 mm off axis (half of the fibers pitch). For the 1×2 switching configuration, the achromat is shifted 0.250 mm off axis, etc.

Fig. 15 shows that every switching configuration has a maximum coupling efficiency corresponding to a specific focal length ($f_{\max}$). For example the 1×3 1-D one-directional configuration has a maximum coupling efficiency of 82% at $f_{\max} = 20$ mm. If $f > f_{\max}$, the coupling efficiency decrease is a consequence of the increase of the aberrations with the focal length, described by (17) and shown in Fig. 9. If $f < f_{\max}$, the coupling efficiency decreases due to the aberrations generated by the larger deflection angle α given by the off-axis position of the lens, as shown in Fig. 16. For a given focal length, addressing fibers further away from the center (for example 1×8) requires larger deflection angles, which generates larger aberrations. For small focal lengths ($f \lesssim 10$ mm) and for receiver fibers which are far away (left bottom grey zone in Fig. 15), the coupling efficiency is affected by a clipping effect. The lateral displacement of the lens is large compared to the diameter of the lens.

For a two-dimensional (2-D) two-direction system (bidirectional displacement of the achromat in the XY plane), the receiver fibers are confined within a circle of radius corresponding to the number of receiver fibers of the 1-D one-directional system (see Fig. 17). The 1-D one-directional

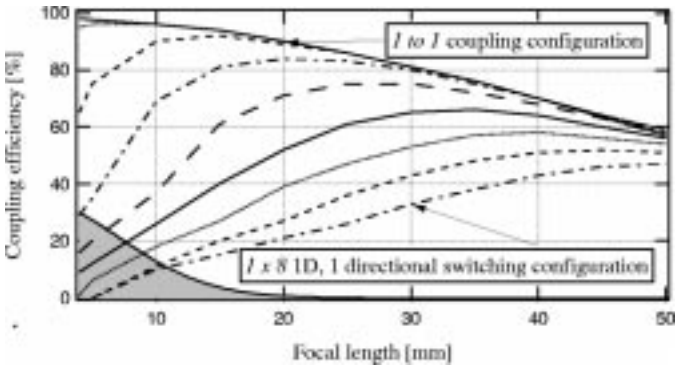

Fig. 15. Coupling efficiency versus focal length for 1-to-1 coupling configuration, and, 1-dimensional, 1-directional switching configurations 1×1, 1×2, 1×3, 1×4, 1×5, 1×6, 1×7 and 1×8 ($NA_{\text{fiber}} = 0.11$, $NA_{\text{lens}} = 0.17$).

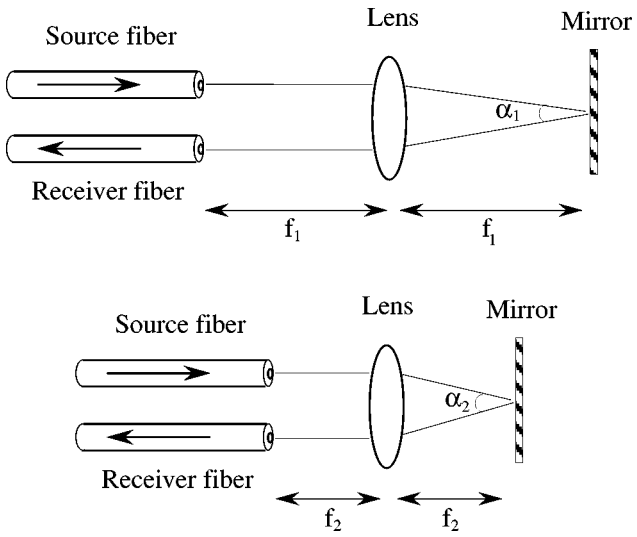

Fig. 16. Geometry for the same switching configuration realized with lenses of different focal lengths f_1 and f_2.

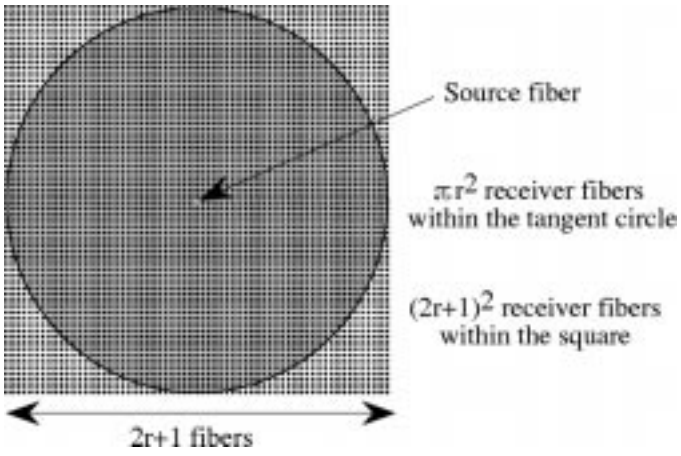

Fig. 17. 2-D arrangement of fibers. r is the number of receiver fibers for the corresponding 1-D one-directional system.

with eight switching configurations for example, corresponds to a 2-D two-direction system with 201 switching configurations.

Fig. 18 shows the coupling efficiency and the standard deviation σ_W of the aberrations as a function of the receiver fiber number (1-D one-directional). The switching system is a 1-D

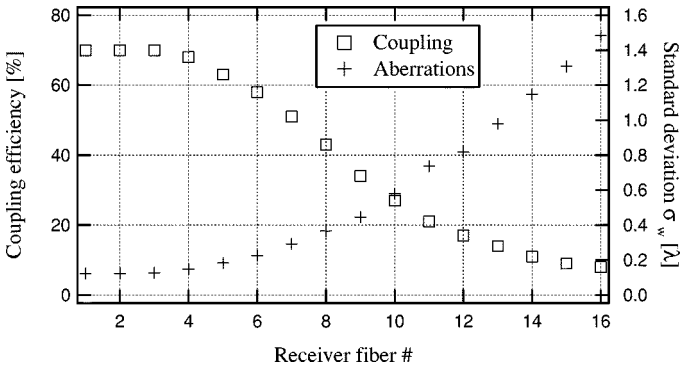

Fig. 18. Coupling efficiency and standard deviation σ_W of the aberrations versus receiver fiber number for a 1-D one-directional $4f$ system with an achromat and a flat mirror as shown in Fig. 14 ($f = 40$ mm, $NA_{\text{fiber}} = 0.11$, $NA_{\text{lens}} = 0.17$).

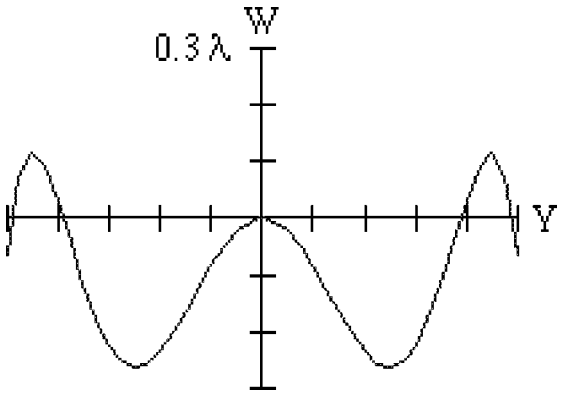

Fig. 19. Optical path difference for the 1-to-1 coupling configuration of the $4f$ system with an achromat on axis versus normalized exit pupil coordinate Y ($f = 40$ mm and $NA = 0.17$).

one-directional $4f$-system with an achromat and a flat mirror, as shown in Fig. 14, for $f = 40$ mm, $NA_{\text{fiber}} = 0.11$, and $NA_{\text{lens}} = 0.17$. Fig. 18 shows that the coupling efficiency decreases rapidly as a function of the receiver fiber number, due to the increasing aberrations. The presented system would allow us to switch between $2 \times 7 = 14$ fibers linearly or to $\pi 7^2 \cong 153$ fibers in two dimensions with insertion loss of less than 3 dB ($\eta = 50\%$).

These results demonstrate that a correction of the aberrations is essential to address a large number of receiver fibers. In the following section, we will present one solution to prevent large aberrations in the system by reducing the employed aperture of the achromat. Other approaches include the use of a deformable mirror to correct for the aberrations [8] or the use of a specially designed holographic optical element (HOE) in order to minimize the aberrations for every configuration. Such an approach has been proposed and investigated [9] for holographic optical scanners.

VIII. Reducing the System Aberrations With Microlenses

In Section VII, the dependance of the aberrations as a function of the numerical aperture NA of the lens has been shown. Larger NA yield larger standard deviations of the aberrations and consequently lower coupling efficiencies. Fig. 19 shows the optical path difference W (referenced to the chief ray) for the 1-to-1 coupling configuration of the $4f$ system with an achromat on axis for a focal length $f = 40$ mm and a numerical aperture $NA = 0.17$.

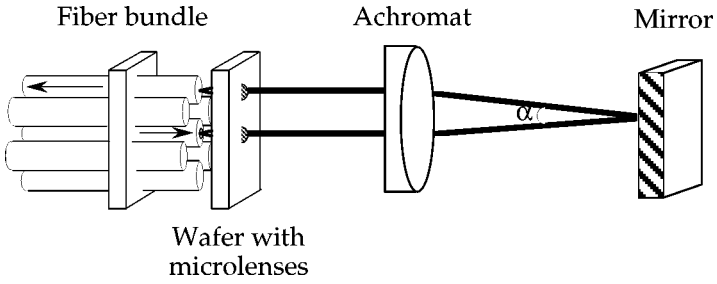

Fig. 20. Schematic setup of the free space switching system using microlenses to reduce the numerical aperture and an achromat to switch from the source fiber to the receiver fibers.

Reducing the numerical aperture by taking only small parts of the lens would reduce the system aberrations.

A. Free Space Switching System With Microlenses

In order to reduce the numerical aperture, we propose placing microlenses on-axis in front of every fiber. Fig. 20 shows the setup of the proposed system. The switching is realized by laterally displacing the achromat. We chose a system with a microlens of diameter $\phi = 245$ μm and $f_{ml} \cong 660$ μm to collimate the Gaussian beam from the source fiber and an achromat of $f = 40$ mm to deflect the light. For fibers with $NA_{\text{fiber}} = 0.11$, the effective aperture of the achromat has a diameter of $0.22 f_{ml} = 145$ μm, which is only 0.8% of the total aperture diameter of the achromat. The beam is focused onto the receiver fibers with identical microlenses. The coupling efficiency has been calculated with the ray tracing program Zemax, as described in Section IV. For singlemode fibers with $NA_{\text{fiber}} = 0.11$, a coupling efficiency of 98% (0.1-dB insertion loss) was found for the 1-to-1 coupling configuration (source and receiver fiber is the same fiber, achromat on-axis). The same coupling efficiency is obtained for switching configurations up to the deflection limit, where the beam is passing just at the edge of the achromat.

B. Alignment Tolerances of the Free Space Switching Optical System With Microlenses

The tolerances for lateral and angular misalignment of the receiver fiber, shown in Fig. 21(b) and (c), are quite the same as the tolerances for the system without microlenses (Figs. 12 and 13, respectively), whereas the tolerance for longitudinal misalignment shown in Fig. 21(a) is more critical than for the system without microlenses (Fig. 11).

The alignment of the microlens array with respect to the fiber array is an additional degree of freedom. However, if the array of microlenses has a lateral offset with respect to the fiber bundle (the offset is the same for every connection), then the system is self-correcting. In the worst case, the deflection generated by the offset of the microlens array makes the beam reach the edge of the achromat or the edge of the mirror, or even worse pass beside the achromat or the mirror. Roughly, a lateral offset of the microlens array is tolerable up to 20% of the radius of the

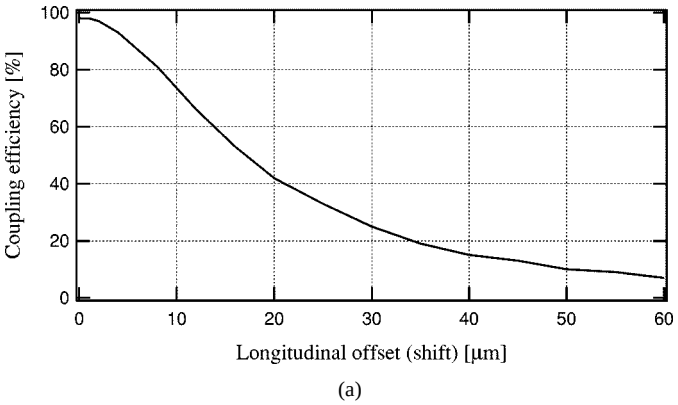

(a)

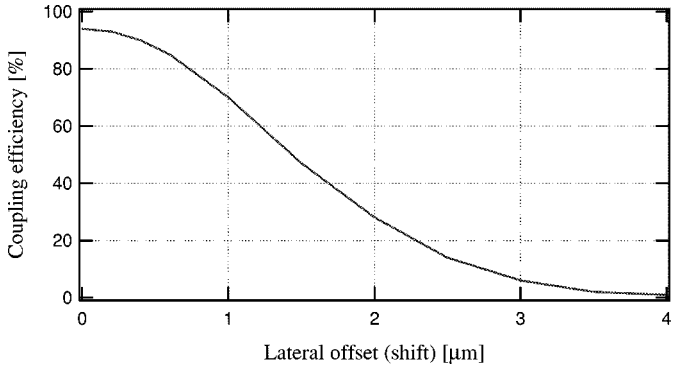

(b)

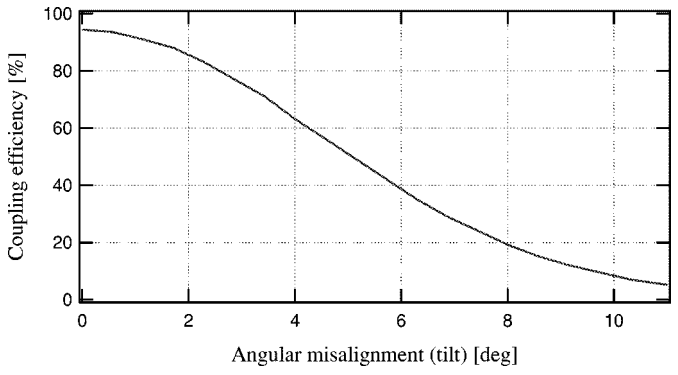

(c)

Fig. 21. $4f$ system with microlenses, achromat, and flat mirror ($NA_{\rm fiber} = 0.11$, $f = 40$ mm): power coupling efficiency versus: (a) longitudinal misalignment, (b) lateral misalignment, and (c) angular misalignment of the receiver fiber.

microlens. For our system, using a microlens with a diameter $\phi = 245$ μm, a lateral offset of the microlens array with respect to the fiber bundle of 26 μm causes 1-dB insertion loss (80% coupling efficiency). A lateral offset of the microlens array is without noticeable influence up to 15 μm.

The lateral misalignment tolerances of the achromat shown in Fig. 22 are less critical than for the system without microlenses. An offset of $\delta x/2$ of the achromat generates an offset of the incoming beam on the microlens of δx which finally results in an angular misalignment $\delta\theta \cong \delta x/f_{ml}$ on the receiver fiber, as shown in Fig. 23. A lateral misalignment of 13 μm of the achromat causes 1-dB insertion loss (80% coupling efficiency). This important result is to compare with the lateral misalignment tolerances of the achromat for the system without microlenses (0.5 μm for 1-dB insertion loss; see Fig. 12). As a

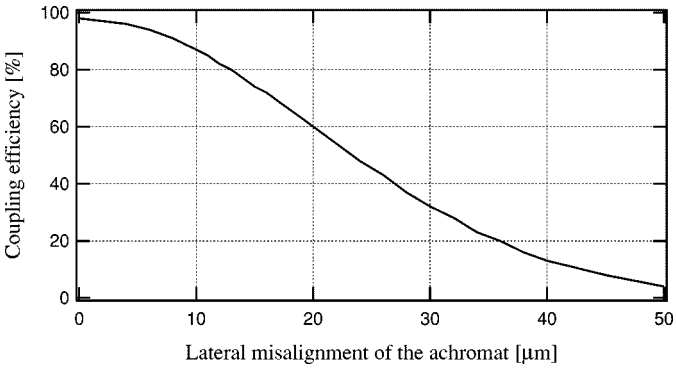

Fig. 22. $4f$ system with microlenses, achromat, and flat mirror: power coupling efficiency versus lateral misalignment of the achromat. ($NA_{\rm fiber} = 0.11$, $f_{\rm achr} = 40$ mm, $f_{ml} = 660$ μm).

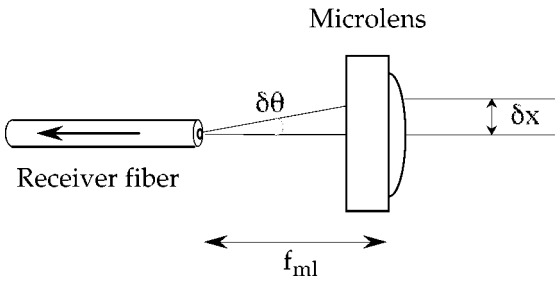

Fig. 23. Schematic of the angular misalignment $\delta\theta = \delta x/f_{ml}$ resulting from a lateral offset $\delta x/2$ of the achromat (not shown in the figure).

reminder, the displacement of the achromat to switch from one position to the next one is 125 μm (see Section VII-C).

We have seen in this section the advantages of using an array of microlenses in front of the array of fibers. The alignment tolerances of the achromat are relaxed and the power coupling efficiency is high due to low aberrations. Nevertheless, the alignment tolerances of each individual receiver fiber are quite severe: 0.7 μm lateral misalignment of one receiver fiber generates 1-dB insertion loss [Fig. 21(b)]. This critical point requires a high precision on both fiber and microlens arrays. The distance between the microlenses is very accurate as the array is fabricated by photolithography (Section VIII-C). The position of the fibers inside the bundle is, however, less accurate. This is due to the eccentricity of the core of the fiber which is in the range of 1 μm and to the positioning of the fiber into the bundle. Although a fiber bundle with lateral alignment tolerances better than 1 μm is possible, to date, no such 2-D singlemode fiber bundles are commercially available. Linear arrays of fibers are, however, commercially available. We will use a linear array of 32 singlemode fibers to demonstrate our switching systems. Fundamentally, there are no more challenges to moving the achromat in both X and Y directions versus in one direction.

C. Fabrication and Characteristics of the Microlenses

In this section, we describe briefly the fabrication process of the plano-convex microlenses and their main characteristics. The microlenses are fabricated by the melting resist technology [10]. A thick layer (1 to 100 μm) of photoresist is spin-coated over a base layer (0.5 to 1 μm), spin-coated on a quartz substrate. After a prebake, the resist is exposed. Photoresist cylin-

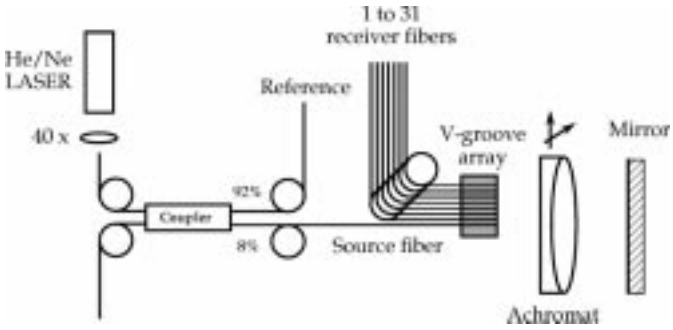

Fig. 24. Experimental setup of the switching system.

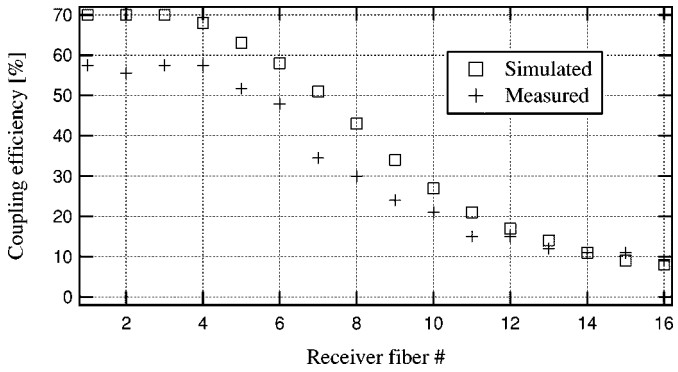

Fig. 25. Measured coupling efficiency using a flat mirror, compared with simulation (Section VII-C).

ders are obtained after standard developing. These cylinders are then melted at a temperature of 150 °C to 200 °C. The resulting structures act like microlenses. A careful optimization of all process steps is necessary in order to obtain a suitable lens profile with a good optical performance.

The microlens is characterized by the radius r and the height h_l at the vertex. The radius of curvature R at the vertex is then [10]

$$R = \frac{h_l}{2} + \frac{r^2}{2h_l} \tag{20}$$

and the focal length is found to be

$$f_{ml} = \frac{R}{n-1} = \frac{h_l + \dfrac{r^2}{h_l}}{2(n-1)} \tag{21}$$

where n is the refractive index of the resist.

In order to characterize the microlenses, several methods are used. The height of the lens and its surface profile are measured using a mechanical profilometer. A Twyman–Green interferometer [11], [12] is used to measure the deviation of the surface profile from an ideal sphere and the radius of curvature R at the vertex. In addition a Mach–Zehnder interferometer (MZI) [11], working in transmission, is used to measure the wave aberrations of the plano-convex microlens.

IX. Experimental Results

The system is composed of one singlemode source fiber placed in the front focal plane of a lens and a mirror placed in the back focal plane, which reflects the light. After passing the lens again, the light is focused into a singlemode receiver fiber located at the same plane as the source fiber. Moving the lens laterally allows us to switch from the source fiber to one of the receiver fibers. The experimental setup is schematically shown in Fig. 24. Light emitted from a He–Ne laser ($\lambda = 633$ nm) is coupled into a singlemode fiber using an aspheric lens. A coupler 92%/8% splits the signal into a reference fiber and a source fiber. The source fiber is part of a linear array of 32 singlemode fibers. The 32 fibers are held in a commercially available (Wave Optics) silicon V-groove array. The distance between adjacent fiber cores is 250 μm $\pm$ 0.5 μm. The singlemode fibers have a cutoff wavelength $\lambda_{\text{cut-off}} = 590$ nm. The mode field diameter is $2w_s = 4.5$ μm, corresponding to a core diameter of $\phi_{\text{core}} = 3.8$ μm and the numerical aperture of $NA_{\text{fiber}} = 0.11$. The cladding diameter is $\phi_{\text{cladding}} = 125$ μm.

The linear array of fibers is placed in the front focal plane of the lens, whereas the mirror is placed in the back focal plane. The lens is an achromat of focal length $f = 40$ mm with an antireflective coating (reflectance $< 0.3\%$). The achromat is a commercially available doublet (Linos #322 209) made of SF2 (n= 1.64 at 633 nm) and BK7 (n= 1.52 at 633 nm). Switching from the source fiber to any of the 31 receiver fibers is possible by moving the achromat laterally using a precision *x–y* stage with a resolution of $\sim$0.14 μm. The signals from the receiver fiber and the reference fiber are detected with calibrated silicon photodiodes. The ratio of the receiver and the reference signal gives the coupling efficiency. The way we use the linear array of fibers, the source fiber at one end, demonstrates the feasibility of a system, which is twice as large with symmetric displacement of the achromat. The 32 fiber linear array can demonstrate the feasibility of a 1×62 1-D system. Moreover, 2-D arrays could be switched if the achromat is displaced in both x and y directions. The 32 fiber linear array can thus demonstrate the feasibility of a 1×3019 2-D system (see Fig. 17).

A. Fiber Switch With a Flat Mirror

In the first system, we use a flat silver-coated mirror with a reflectivity of 96%. The surface quality is better than $\lambda/10$. Switching from the source fiber to any of the 31 receiver fibers is obtained by moving the achromat laterally with the precision *x–y* stage (see Fig. 24). The coupling efficiency is optimized by adjusting the distance between the fiber holder and the achromat for every connection. Fig. 25 shows the measured coupling efficiency, together with the calculated values (see Section VII-C). The total losses due to the optical elements are estimated to be 14%, by taking into account 4% Fresnel losses at the interfaces of the source and the receiver fiber, 1% transmission loss for the achromat and 0.3% reflectance at both interfaces, and 96% reflectivity for the mirror. Fig. 25 shows the coupling efficiency for 1-D one-directional 1×16 switching. The measured coupling efficiency decreases with increasing distance between the source fiber and the receiver fibers, as predicted by the simulations. This decrease is due to the aberrations of the system described in Section VII. These results demonstrate the limit for such an optical switch without further aberration correction. Six receiver fibers can be addressed with a coupling efficiency better than 50% (less than 3-dB insertion loss) without the 14%

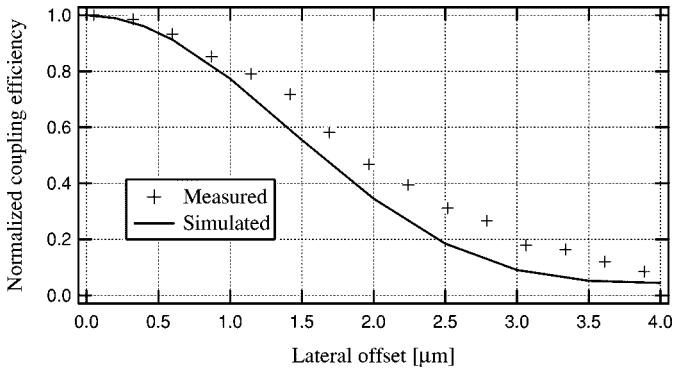

Fig. 26. Measured coupling efficiency for a lateral offset of the receiver fiber, compared with simulation (Section VII-B).

residual losses. A corresponding 2-D system with less than 3-dB insertion loss could address 113 receiver fibers (quadratic array of fibers encircled in a radius of 6 fibers, see Fig. 17).

The tolerances for a lateral offset of the receiver fiber are also measured and the result is shown in Fig. 26.

These measured tolerances are in good agreement with the simulated ones (see Section VII-B). For high efficiency, an accuracy of 0.5 μm is required for the position of the receiver fiber. A lateral misalignment of the achromat produces a lateral misalignment of the beam on the receiver fiber twice as large. Therefore, the required accuracy for the position of the achromat is 0.25 μm.

B. Fiber Switch Using Microlens Arrays

In Section IX-A, the limit of the optical switch using an achromat and a flat mirror has been demonstrated. In the present section, we investigate another way to reduce the aberrations. As described theoretically in Section VII, the aberrations are proportional to the power four of the numerical aperture of the system. In order to reduce the effective aperture of the achromat, we propose placing a microlens in front of each source and receiver fiber (see Fig. 20). The function of the microlens placed at the output of the source fiber is to collimate the beam. The microlenses placed in front of the receiver fibers focuses the beam into the fiber core. The switching function is done by a lateral displacement of the achromat.

We use a microlens fabricated by the melting resist technology (see Section VIII-C) with a diameter $\phi = 245$ μm. The measured height at the vertex is $h_l = 23.6$ μm. The focal length is calculated by (21) as $f_{ml} \simeq 660$ μm. The microlens aberrations of the illuminated disc ($\phi = 94$ μm) were measured with a MZI (see Section VIII-C). The measured standard deviation of the aberrations [see (18)] is $\sigma_W = 0.02\lambda$, which corresponds to a Strehl ratio of $0.98 \cong \eta$. The quality of the microlens is then very good. Almost no losses are generated by the aberrations of the microlens. The experimental setup of the switching system is shown in Fig. 27. The wafer with the array of microlenses is placed in front of a V-groove array, containing the fibers, and is adjusted using a *x–y–z* stage (1-μm resolution). The lateral displacement of the achromat allows us to switch the 31 receiver fibers. The collimated beam is focused onto the flat mirror. The system allows us to switch the signal from the source fiber, up to

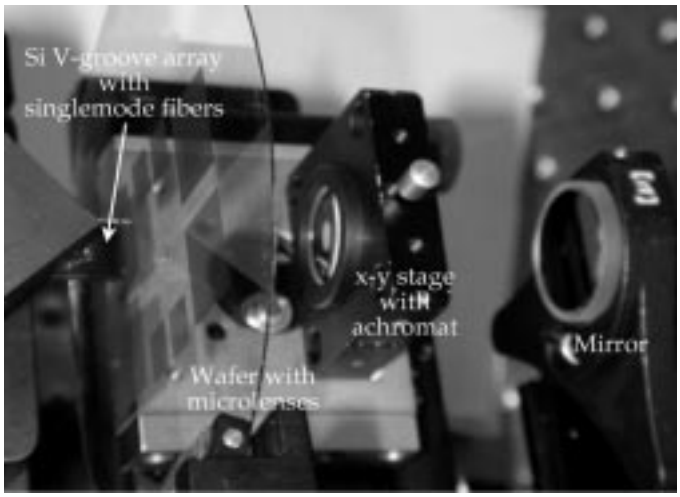

Fig. 27. Experimental setup of the switching system using a microlens array.

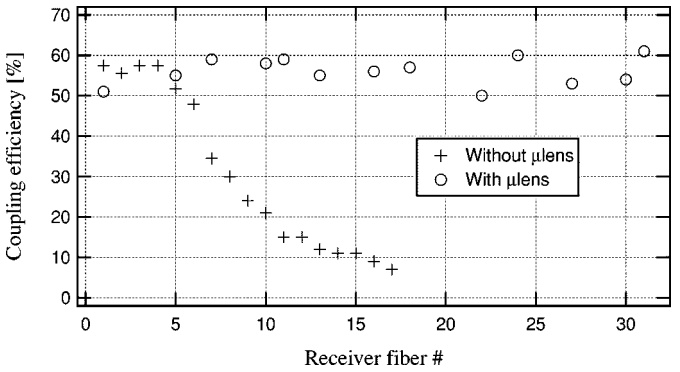

Fig. 28. Measured coupling efficiency using microlens arrays, compared with the flat mirror (Section IX-A).

the 31st fiber with a coupling efficiency between 50% and 61%, as shown in Fig. 28. The total loss due to the optical elements is estimated to be 36%, by considering two interfaces between the microlens and air (index matching oil is used between the fibers and the wafer with the microlenses, see Fig. 20), with 4% Fresnel losses each, 14% transmission loss inside the photoresist microlens, 1% transmission loss inside the achromat and 0.3% of reflectance at both interfaces, and a reflectivity of 96% for the mirror. The theoretical maximum efficiency is 98% (see Section VIII-A). If we add the losses due to the optical elements (36%) to the maximum measured coupling efficiency (61%), we almost reach the theoretical limit. Cross talk is less than -30 dB (detection limit).

The resist is a material which degrades with time. It has to be replaced by other materials which are more stable and have less absorption (resist has 14% absorption at $\lambda = 0.633$ μm). The resist microlenses can be transferred into different materials by reactive ion etching (RIE) [5]. The choice of the material is wavelength dependent. Fused silica is used for applications with UV light to visible and silicon is used for IR applications.

The measured coupling efficiency as a function of the lateral offset of the achromat is shown in Fig. 29. These measured tolerances are less critical then the simulated ones (see Section VIII-B, Fig. 22). This is probably due to a slight defocus

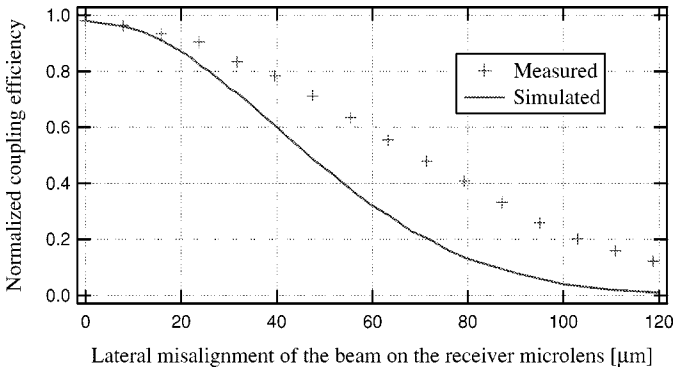

Fig. 29. Measured coupling efficiency for a lateral misalignment of the beam on the receiver microlens, compared with simulation (Section VIII-B, Fig. 22).

of the microlens which generates a wider spot on the fiber. For high efficiency, an accuracy of the achromat of 10 μm is required. Compared to the switching system without microlens arrays (see Section IX-A, Fig. 26), which requires 0.25- μm accuracy on the position of the achromat for high efficiency, the system using microlenses is much less critical.

The use of microlenses gives high coupling efficiency with relaxed tolerances of the alignment for the incoming beam on the receiver microlens. The alignment of the linear fiber array with the microlens array is realized with a precision *x–y–z* stage (1 -μm resolution). The reported results indicate that the alignment of the microlens array with the fiber array is possible. Several alignment schemes using a microoptical bench have been proposed to align plano-convex microlenses with singlemode fibers placed in V-grooves [13], [14]. These solutions, however, remain one dimensional.

X. Conclusion

Detailed investigations on optical switches for a large number of interconnects have been carried out. Several issues have been pointed out and correlating experiments have been shown. The feasibility of an optical switching system using microlenses for a large number of interconnects has been demonstrated theoretically as well as experimentally. Insertion loss as low as 1 dB (80% coupling efficiency) is almost possible. The use of IR light ($\lambda = 1.55$ μm) instead of red light ($\lambda = 0.633$ μm) would even relax the alignment tolerances. In fact, the diameter of the core of singlemode fibers is around 10 μm for $\lambda = 1.55$ μm and around 4 μm for $\lambda = 0.633$ μm.

Other approaches to replace the array of microlenses have been reported. The fabrication of a lens directly on top of the fiber as was proposed for laser to fiber coupling by [15] and [16] (arc discharge machining), and by [17] and [18] (laser micromachining). Nevertheless, the surface of such microlenses is difficult to fabricate accurately. Moreover, an accurate control of the height of the lens is not possible. As the focal length depends on the height of the lens, homogenous lensed fibers array is not possible with these techniques. Another approach is possible using graded-index (GRIN) fiber lenses as proposed by [19]–[21].

Compared to these other approaches, the arrays of microlenses fabricated by the melting resist technology have the advantage of a high homogeneity of the surface quality and of the focal length.

Acknowledgment

The authors would like to thank K. Weible (Weible OpTech) and I. Philipoussis for the fabrication of microlenses.

References

[1] D. J. Bishop, C. R. Giles, and S. R. Das, "The rise of optical switching," *Scientific Amer.*, vol. 284, no. 1, pp. 88–94, Jan. 2001.
[2] C. Marxer and N. F. de Rooij, "Micro-opto-mechanical 2×2 switch for single-mode fibers based on plasma-etched silicon mirror and electrostatic actuation," *J. Lightwave Technol.*, vol. 17, pp. 2–6, Jan. 1999.
[3] J. W. Goodman, *Introduction to Fourier Optics*, 2nd ed. New York: McGraw-Hill, 1996.
[4] D. Marcuse, "Loss analysis of single-mode fiber splices," *Bell Syst. Tech. J.*, vol. 56, no. 5, pp. 703–718, 1977.
[5] H. P. Herzig, Ed., *Micro-Optics*. London, U.K.: Taylor & Francis, 1997.
[6] W. T. Welford, *Aberrations of Optical Systems*. Bristol, U.K.: Adam Hilger, 1986.
[7] W. J. Smith, *Modern Optical Engineering*, 2nd ed. New York: McGraw-Hill, 1990.
[8] Y.-A. Peter, F. Gonté, H. P. Herzig, and R. Dändliker, "Micro-optical fiber switch for a large number of interconnects using a deformable mirror," IEEE Photon. Technol. Lett., to be published.
[9] H. P. Herzig and R. Dändliker, "Holographic optical scanning elements: Analytical method for determining the phase function," *J. Opt. Soc. Amer. A*, vol. 4, no. 6, pp. 1063–1070, 1987.
[10] Ph. Nussbaum, R. Völkel, H. P. Herzig, M. Eisner, and S. Haselbeck, "Design, fabrication and testing of microlens arrays for sensors and microsystems," *Pure Appl. Optics*, vol. 6, pp. 617–636, 1997.
[11] M. Born and E. Wolf, *Principles of Optics*, 6th ed. Cambridge, U.K.: Cambridge Univ. Press, 1999.
[12] J. Schwider and O. Falkenstörfer, "Twyman–Green interferometer for testing microspheres," *Optical Eng.*, vol. 34, no. 10, pp. 2972–2975, 1995.
[13] H. Kiessling, U. Danzer, and J. Schwider, "Monomode fiber-array connectors," Annual Rep., Universität Erlangen-Nürnberg, 1996.
[14] Y. Aoki, T. Kato, R. J. Mizuno, and K. Iga, "Micro-optical bench for alignment-free optical coupling," *Appl. Opt.*, vol. 38, no. 6, pp. 963–965, 1999.
[15] H. Kuwahara, M. Sasaki, and N. Tokoyo, "Efficient coupling from semiconductor lasers into single-mode fibers with tapered hemispherical ends," *Appl. Optics*, vol. 19, no. 15, pp. 2578–2583, 1980.
[16] J.-I. Yamada, Y. Murakami, J.-I. Sakai, and T. Kimura, "Characteristics of a hemispherical microlens for coupling between a semiconductor laser and single-mode fiber," *IEEE J. Quantum Electron.*, vol. 16, pp. 1067–1072, 1980.
[17] H. M. Presby, A. F. Benner, and C. A. Edwards, "Laser micromachining of efficient fiber microlenses," *Appl. Opt.*, vol. 29, no. 18, pp. 2692–2695, 1990.
[18] C. A. Edwards, H. M. Presby, and C. Dragone, "Ideal microlenses for laser to fiber coupling," *J. Lightwave Technol.*, vol. 11, pp. 252–257, Feb. 1993.
[19] W. L. Emkey and C. A. Jack, "Analysis and evaluation of graded-index fiber-lenses," *J. Lightwave Technol.*, vol. LT-5, pp. 1156–1164, 1987.
[20] P. Chanclou, M. Thual, J. Lostec, D. Pavy, M. Gadonna, and A. Poudoulec, "Collective microoptics on fiber ribbon for optical interconnecting devices," *J. Lightwave Technol.*, vol. 17, pp. 924–928, May 1999.
[21] P. Chanclou, M. Thual, J. Lostec, D. Pavy, and M. Gadonna, "Focusing and coupling properties of collective micro-optics on fiber ribbons," *Opt. Eng.*, vol. 39, no. 2, pp. 387–392, 2000.

Yves-Alain Peter received the diploma in physics, in 1994, and the Ph.D. degree, in 2001, both from the University of Neuchâtel, Switzerland.

In 1995, he was a Scientific Collaborator with the Medical Radiobiology Department of the Paul Scherrer Institute in Villigen, Switzerland, and joined the Applied Optics Group at the Institute of Microtechnology of the University of Neuchâtel, Switzerland, as a Ph.D. student and Teaching Assistant. He is now a Postdoctoral Researcher with the Microphotonics group at Stanford University, Stanford, CA. His current research interests include micro-opto-electro-mechanical systems with applications in adaptive optics and optical switching.

Dr. Peter is member of IEEE/LEOS, Optical Society of America, and the Swiss Physical Society.

Hans Peter Herzig received the diploma in physics from the Swiss Federal Institute of Technology, Zürich, Switzerland, in 1978. In 1987, he received the Ph.D. degree in optics from the University of Neuchâtel, Switzerland.

From 1978 to 1982 he was a Scientist with the Optics Development Department of Kern in Aarau, Switzerland, working in lens design and optical testing. In 1983, he became a Graduate Research Assistant with the Applied Optics Group at the Institute of Microtechnology of the University of Neuchâtel, Switzerland, working in the field of holographic optical elements, especially scanning elements. He currently heads the micro-optics research group and is an Associate Professor at the University of Neuchâtel.

Dr. Herzig is member of Optical Society of America, European Optical Society, and the German Society of Applied Optics, and a board member of the Swiss Society of Optics and Microscopy.

René Dändliker was born in Zug, Switzerland, in 1939. He received the Diploma in physics from the Swiss Federal Institute of Technology, Zürich, Switzerland, in 1963, the Ph.D. degree in physics from the University of Berne, Switzerland, in 1968, and the Venia Legendi for applied physics at the Swiss Federal Institute of Technology, Zürich, in 1978.

From 1963 to 1969 he was Graduate Research Assistant at the Institute of Applied Physics, University of Berne, where he worked on gas and solid-state lasers. From 1969 to 1970 he was Research Scientist at the Philips Research Laboratories, Eindhoven, The Netherlands, in the field of applied optics. From 1970 to 1978 he was Senior Scientist and Head of the Coherent Optics Group at the Brown Boveri Research Center, Baden, Switzerland, where he was concerned with optical metrology applied to mechanics, such as laser Doppler velocimetry and heterodyne holographic interferometry. Since 1978 he has been Professor of Applied Optics at the University of Neuchâtel, Switzerland, and since 1989 also a Professor of Applied Optics at the Swiss Federal Institute of Technology, Lausanne. His current research activities include optical metrology, optical fibers and sensors, holography and optical computing, diffractive optical elements, and micro-optics.

Dr. Dändliker served the European Optical Society (EOS) as President from 1994 to 1996. He is a Vice-President of the International Commission for Optics (ICO), a fellow of the OSA and the Swiss Academy of Engineering Sciences (SATW), a member of the SPIE, the French Society of Optics (SFO), the German Society of Applied Optics (DGaO), and the European Physical Society (EPS), and an affiliate of LEOS/IEEE.